PARP Inhibitor Olaparib Enhances the Efficacy of Radiotherapy on Xrcc2-deficient Colorectal Cancer Cells

changjiang Qin (10220037@vip.henu.edu.cn)
Department of Gastrointestinal Surgery, Huaihe Hospital of Henan University, Kaifeng, China
Zhi-Yu Ji
Henan University
Er-Tao Zhai
Sun Yat-Sen University
Kai-Wu Xu
Sun Yat-Sen University
Quan-Ying Li
Henan University
Hong Jing
Henan University
Yi-Jie Zhang
Henan University
Xin-Ming Song
Sun Yat-Sen University

Research

Keywords: XRCC2, PARP□Colorectal Cancer, Radiotherapy

Posted Date: March 30th, 2021

DOI: https://doi.org/10.21203/rs.3.rs-341240/v1

Abstract

Background: Loss of XRCC2 compromises DNA damage repairs, and induced DNA damage burdens may increase the reliance on PARP-dependent DNA repairs of cancer cells to render cell susceptibility to PARP inhibitor therapy. Here, we study if XRCC2 loss sensitizes colorectal cancer(CRC) to PARP inhibitor in combination with radiotherapy (RT).

Methods: The relationships between the expression of XRCC2 and PARP with patient outcome were investigated in 167 patients with locally advanced rectal cancer (LARC) who received neoadjuvant chemoradiotherapy (neoCRT). The *in vitro* radiosensitizing effects of olaparib were tested in *XRCC2*-deficient CRC using a clonogenic survival assay, determination of γH2AX foci, and measurement of β-galactosidase activity. An *in vivo* mouse xenograft model was used to determine the effect of olaparib on sensitization of tumors to ionizing radiation (IR).

Results: High levels of XRCC2 or PARP1 were significantly associated with poor overall survival (OS) in patients with LARC who received neoCRT, co-expression analyses found low PARP1 and low XRCC2 expression have better OS. Our *in vitro* experiments indicated that olaparib+IR reduced clonogenic survival, increased persistent DNA damage, and prolonged cell cycle arrest and senescence in *XRCC2*-deficient cells relative to wild-type cells. Furthermore, our mouse xenograft experiments indicated that RT+olaparib had greater anti-tumor effects and led to long-term remission in mice with *XRCC2*-deficient tumors.

Conclusions: *XRCC2*-deficient CRC acquire high sensitivity to PARP inhibition after IR treatment. Our preclinical findings provide a rationale for the use of Olaparib as a radiosensitizer for treatment of *XRCC2*-deficient CRC.

Background

Colorectal cancer (CRC) is one of the most common malignancies and a leading cause of cancer-related death worldwide (1). The National Comprehensive Cancer Network (NCCN) guidelines recommend neoadjuvant radiotherapy/chemoradiotherapy (neoRT/CRT) as the standard treatment for patients with locally advanced rectal cancer (LARC) because it can significantly increase local control and cancer-specific survival (2, 3). Most LARC patients treated with neoRT/CRT exhibit some degree of tumor response, but other patients experience resistance to this therapy. An increasing number of investigations reported that the response of individual CRC patients to this treatment is associated with gene expression patterns in cancer cells (4). The X-ray repair complementing defective repair in Chinese hamster cells 2 gene (*XRCC2*) codes for a DNA repair protein, and its expression in some cancers is associated with increased radioresistance. For example, our previous study showed that 72% of LARC patients who tested negative for XRCC2 expression in cancer tissues had good pathologic responses and prognoses following neoRT; however, the other 28% of patients who tested negative for XRCC2 developed radioresistance and had poor prognoses (5). It seems possible that when cancer cells lose XRCC2

function, they develop an alternative or compensatory pathway(s) for DNA repair. Therefore, agents that specifically target and radiosensitize tumor cells may be an effective treatment for patients with radioresistant tumors. For example, tumor cells that have BRCA-inactivation are sensitive to poly (ADP-ribose) polymerase (PARP) inhibition due to their deficiency in homologous recombination repair (HRR) (6,7).

RT kills cancer cells mostly through by induction of various forms of DNA damage, and double-strand breaks (DSBs) are the most toxic type of DNA damage (8). Cells repair DSBs *via* two main pathways: non-homologous end-joining (NHEJ) and homologous recombination repair (HRR) (9). PARP1 plays an important role in the sensing and initiation of DNA repair, and functions in most forms of DNA repair, including repair of single strand breaks (SSBs) and DSBs (10). Because of the essential role of PARP in recognition and repair of DSBs, researchers used PARP inhibitors to sensitize tumors defective in HRR following induction of DSBs with ionizing radiation (IR), and reported the accumulation of DNA DSBs and cell death (11-13).

HRR activity in tumor cells is a key factor for predicting whether treatment with a PARP1 inhibitor will be successful (14). The XRCC2 protein is a key factor in HRR, and it contributes to the repair of DSBs (15, 16). Our previous studies showed that inhibition of XRCC2 sensitized CRC cells to radiation by inhibition of HRR (5). This led us to hypothesize that a PARP1 inhibitor has potential for use as a radiosensitizer to enhance the therapeutic effect of RT in XRCC2-deficient CRC. Therefore, the present study of *in vitro* and *in vivo* models evaluated the radiosensitizing effect of olaparib, a drug approved for the treatment of several cancers with BRCA mutations, on CRC cancers that have different XRCC2 status. We found that olaparib produced highly significant radiosensitization in XRCC2-deficient CRC. Analysis of the contributions of DNA repair and senescence to the radiosensitization revealed that XRCC2-deficient cells incur significantly more DNA damage and senescence in vitro and in vivo. Therefore, we believe that our results support further clinical trials with olaparib and radiotherapy for XRCC2-deficient CRC.

Methods

Patients

A total of 167 LARC patients were examined. All patients had newly diagnosed LARC and received neoCRT from January 2010 and December 2016 at The First Affiliated Hospital (Sun Yat-sen University) and Huaihe Hospital (Henan University). The inclusion criteria were presence of a single primary lesion, completion of standard neoCRT and receipt of radical surgical resection, and completion of adjuvant chemotherapy with a capecitabine, XELOX, or mFOLFOX6 regimen. Biopsy tissue samples were obtained from all patients before administration of neoCRT (5). The use of tissue blocks was approved by the Institutional Ethics Review Board of the Huaihe Hospital of Henan University and the First Affiliated Hospital of Sun Yat-sen University, and written consent was obtained from each patient.

Cell lines

The HCT116 and SW480 human CRC cell lines were purchased from American Type Culture Collection (ATCC, Manassas, VA, USA) and cultured according to ATCC guidelines. These cell lines were authenticated by short tandem repeat analysis at the China Center for Type Culture Collection (Wuhan, China). CRC cells with stable knockdown of *XRCC2* (Sh-XRCC2) and with nonsilencing (vector) shRNAs were generated as previously described (5, 17). The knockdown efficiency of *XRCC2* was determined using quantitative RT-PCR and western blotting.

Western blotting

Proteins were separated using 8–10% SDS-PAGE and then electrotransferred to PVDF membranes (Millipore, Billerica, MA, USA). The membranes were blocked for 1 h with 5% bovine serum albumin (BSA; Beyotime, Beijing, China) in TBS-T, and incubated with specific primary antibodies overnight at 4°C, followed by incubation with rabbit or mouse horseradish peroxidase-coupled secondary antibodies for 1 h. Antibody binding was detected using an enhanced chemiluminescence reagent (Millipore, Billerica, MA, USA).

Quantitative real-time PCR

Total RNA was extracted and qRT-PCR was performed as described previously (5, 17). All experiments were performed at least 3 times.

Immunofluorescence

Cells in confocal dishes were fixed in 4% paraformaldehyde, permeabilized using 0.5% Triton X-100, and blocked with 3% BSA. The cells were then incubated with anti-γH2AX (1:50, D17A3, Cell Signaling Technology [CST], Danvers, MA, USA) antibodies at 4°C overnight, followed by incubation with DyLight 488 AffiniPure Goat Anti-rabbit IgG (1:200, Abbkine, Redlands, CA, USA) for 1 h at room temperature in the dark. The samples were then costained with 4',6-diamidino-2-phenylindole (DAPI) and examined by confocal laser scanning microscopy. In each sample, the number of foci of γH2AX (a marker of DSBs) per nucleus was counted using a confocal microscope (Zeiss, Germany), and an average of 100 nuclei were analyzed for each sample.

Clonogenic cell survival assay

The clonogenic survival assay was performed as previously described (5). Briefly, cells were trypsinized to a single-cell suspension and then seeded into 6-well plates for 24 h before treatment. After addition of vehicle (Dimethylsulfoxide [DMSO]) or olaparib for 6 h, a varying dose of IR was applied (0–8 Gy), and the cells were then maintained in an incubator at 37°C with 5% CO2 for 10 to 14 days. The colonies were fixed with methanol and stained by crystal violet and colonies containing more than 50 cells were counted. All experiments were performed in triplicate and repeated three times.

Flow cytometry

For cell cycle analysis, cultured cells were harvested 72 h after treatment, fixed overnight with ice-cold 70% ethanol at −20°C, and then stained with 20 mg/mL propidium iodide (PI) staining buffer (1% Triton X-100 and 100 mg/mL RNase A) for 30 min. DNA content was determined using a FACSCalibur unit (Becton Dickinson, Franklin Lakes, NJ, USA) with ModFit LT version 2.0 software. All experiments were repeated at least three times.

Senescence-associated β-galactosidase assay

A kit for staining cell senescence using β-galactosidase (β-gal) was purchased from CST (#9860), and cells were fixed and stained according to the manufacturer's protocol. For the *in vivo* study, frozen sections of xenograft tumors (5-μm thick) were fixed in 2% glutaraldehyde and stained as in the *in vitro* experiments described above. Five images of stained cells from random fields were recorded using an inverted microscope, and blue-stained senescent cells and unstained cells in each image were counted using a computer. The positive percentages were calculated and presented using GraphPad Prism version 8.0.

Immunohistochemistry

IHC assays were performed as previously described (18). Briefly, 4-μm thick formalin-fixed, paraffin-embedded tissue sections were deparaffinized and rehydrated, followed by antigen retrieval and endogenous peroxidase inactivation. After blocking, the slides were incubated overnight at 4°C with anti-XRCC2 (1:200, #ab180752; Abcam), anti-PARP1 (1:200; #ab32138; Abcam), anti-Ki67(1:300; #9449; Cell Signaling Technology), or anti-γH2AX (1:100; D17A3; Cell Signaling Technology) antibodies and then with secondary antibodies (Vectastain ABC kit). Slides were stained with 3, 3-diaminobenzidine (DAB) and counterstained with hematoxylin.

Animals and in vivo studies

All animal experiments were approved by the Henan University Animal Care and Use Committee. Xenograft experiments were performed as previously described (19). Briefly, 6×10^6 SW480 cells were suspended in 100 μL of PBS and implanted subcutaneously into the right flanks of female BALB/c nude mice (4–5 weeks old, 15–18 g; SLRC Laboratory Animal Co). When the tumors had volumes of approximately 100 mm^3, mice were randomized into four groups: DMSO, olaparib, RT+DMSO, or RT+olaparib. Mice received DMSO or olaparib *via* oral gavage once per day for 12 consecutive days. Mice in the RT+DMSO and RT+olaparib groups received fractionated radiotherapy (2 Gy every other day for 5 days) at 1 h after oral gavage; a lead plate was used for coverage to assure that IR was only applied to the xenograft region. Tumor growth was recorded using a digital caliper, and tumor volume was calculated as: $0.52 \times width^2 \times length$. Mice were euthanized and tumors were harvested 2 days after the last dose of olaparib or oralipib+RT. For long-term studies, mice received oralipib+RT therapy and were monitored for tumor growth until 30 days after RT.

Statistical analysis

One-way and two-way ANOVA tests were used for comparisons in the *in vitro* and *in vivo* experiments, and correction for multiple comparisons was performed using the Tukey or Sidak test, as appropriate. All values are expressed as means ± standard deviations (SDs). A *P*-value of less than 0.05 was considered statistically significant. All statistical analyses were performed using GraphPad Prism version 8.0.

Results

High expression of XRCC2 and PARP1 is associated with poor prognosis in LARCpatients who received neoRT

Our previous research showed that XRCC2 expression in pretreatment biopsy specimens was associated with response to neoRT in LARC patients (5), and that greater expression of *XRCC2* was associated with reduced sensitivity to PARP1 inhibition (20). We therefore investigated the relationship of XRCC2/PARP1 coexpression with the efficacy of RT in patients with LARC.

The expression of XRCC2 and PARP1 in pretreatment biopsy tumor specimens from 167 LARC patients who received neoCRT followed by surgery indicated that 57 samples (34.1%) were $XRCC2^{+}$ and 52 samples (31.1%) were $PARP1^{+}$ (Figure 1A). Kaplan-Meier survival analysis (Figure 1B & C) indicated poor overall survival (OS) in patients with high levels of XRCC2 (P = 0.006) or PARP1 (P = 0.0001). XRCC2/PARP1 coexpression analysis in the whole cohort indicated that patients who had tumors with low coexpression had better OS (P = 0.002; Figure 1D). These data suggest that simultaneous targeting of XRCC2 and PARP1 could be a promising treatment for selected LARC patients. We therefore examined the potential of this treatment regimen using *in vitro* and animal studies.

PARP-1 inhibitor increases radiosensitivity of XRCC2-deficient CRC cells

Our previous studies established a line of colorectal cancer cells with knockdown of *XRCC2* (5, 17). We first confirmed knockdown of XRCC2 in these cells using western blotting (Figure 2A) and qRT-PCR (Figure 2B). We then evaluated the effects of olaparib (a PARP inhibitor) and IR dose on survival of these cells using the clonogenic survival assay (Figure 2C & D). Olaparib+IR significantly reduced colony formation in both cell lines compared to IR alone (all $P < 0.05$), indicating that olaparib radiosensitized these CRC cells. Importantly, relative to cells with empty vectors, *XRCC2*-deficient cells were more sensitive to IR and had higher levels of olaparib-mediated radiosensitization.

Olaparib+IR increases DNA damage in XRCC2-deficient CRC cells

DSBs caused by IR result in rapid production of γH2AX, a marker of impaired cellular capacity to repair DSBs (21, 22). To investigate the effects of olaparib on IR-induced DNA damage, we used immunofluorescence to measure γH2AX in *XRCC2*-deficient CRC cells. The results indicated that treatment with olaparib alone for 48 h did not cause any significant DNA damage, and that treatment with olaparib+IR led to increased levels of γH2AX at 48 h after IR (Figure 3A & B). Importantly, irradiated *XRCC2*-deficient cells had more γH2AX foci than XRCC2-expressing CRC cells at 48 h when treated with

olaparib. These data suggest that treatment with olaparib+IR led to more DNA damage in *XRCC2*-deficient CRC cells than in control cells with empty vectors.

Olaparib promotes G2/M phase arrest in XRCC2-deficient CRC cells after RT

Sustained G2/M growth phase arrest is a classic cellular response to DNA damage (23). Thus, we examined the effect of olaparib with IR on the percentage of *XRCC2*-deficient CRC cells in the G2/M phase. In particular, we performed FACS analysis of CRC cells that had empty vectors and CRC cells with *XRCC2* depletion that were treated with olaparib, IR, or both (Figure 4). The results showed that treatment with olaparib alone did not increase the number of *XRCC2*-deficient cells in phase G2/M. However, IR with olaparib led to significant arrest of the cell cycle at the G2/M phase in both cell lines ($P < 0.01$; Figure 3A & B). Furthermore, olaparib with IR increased the percentage of cells in phase G2/M in *XRCC2*-deficient CRC cells compared to CRC cells with empty vectors ($P < 0.01$; Figure 4A & B).

Olaparib accelerates senescence when combined with IR in XRCC2-deficient cells

Irreversible cell-cycle arrest is a key feature of accelerated senescence. Thus, we analyzed the effect of different treatments on cell senescence using a β-gal assay (Fig. 5A). IR combined with olaparib significantly increased the proportion of β-gal-positivity in *XRCC2*-deficient CRC cells compared with CRC cells that had empty vectors ($P < 0.001$; Fig. 5B). DNA-damaging agents primarily promote senescence *via* the p53/p21 signaling pathway (24), so we also analyzed the effects of different treatments on the levels of phospho-p53 and p21. *XRCC2*-deficient cells and cells with empty vectors had increased levels of phospho-p53 and p21 at 48 h after 10 Gy of IR, and olaparib treatment increased this effect. Moreover, the combined treatment led to higher levels of phospho-p53 and p21 in *XRCC2*-deficient cells than cells with empty vectors (Fig. 5C). These results demonstrate that olaparib enhanced the effect of IR by inducing cell senescence.

Olaparib increases the radiosensitivity of XRCC2-deficient cells in a mouse xenograft model

We also evaluated the effect of irradiation on olaparib sensitivity using mice xenograft experiments in which the two SW480 cell lines only differed in *XRCC2* status (Fig. 6A). Strikingly, olaparib with RT prevented the growth of *XRCC2*-deficient tumors, and was more effective than either treatment alone (Fig. 6B). We also determined whether the combination treatment led to long-lasting effects by following mice that received the combination therapy for two weeks after the final treatment (total duration of 30 days). The results indicated that *XRCC2*+/+ tumors regrew quickly after cessation of therapy, whereas sh*XRCC2* tumors continued to shrink (Fig. 6C).

We assessed the generalizability of these findings by harvesting tumors from all mice 2 days after the last treatment (Fig. 6A). The results indicated that the γH2AX expression of tumor tissues in the olaparib+RT group was significantly greater in *XRCC2*-deficient CRC cells (Fig. 6D). Although there was negligible staining in mice treated with olaparib alone, there was a striking increase in β-gal activity when olaparib was combined with RT, especially in *XRCC2*-deficient CRC cells (Fig. 6F). This coincided with a

marked reduction in cellular proliferation (Ki67 positivity; Fig. 6E). The results of these xenograft tumor model experiments confirmed that olaparib increased the radiosensitivity of *XRCC2*-deficient CRC cells.

Discussion

PARP1 inhibitors are therapeutic agents capable of inducing synthetic lethality in tumors with deficiencies in HR-mediated DNA repair, such as those with BRCA1 mutations (25). Thus, CRC cells that respond to PARP1 inhibitors are likely carry defects in DSB repair enzymes even though BRCA mutations are rare in patients with CRC (26). Previously, we showed that *XRCC2*-deficient CRC cells were sensitive to 5-fluorouracil (5FU) and RT (5, 17). In particular, our study of 67 LARC patients treated with neoRT between 2010 and 2012 indicated that XRCC2 overexpression was associated with RT resistance and poor OS (5). We expanded this cohort to include an additional 100 patients with LARC who were treated from 2013 to 2016, and described the results of all 167 patients herein. Our analysis of these 167 patients confirmed our previous observations. We also found that PARP1 overexpression was negatively associated with OS, and co-expression analyses indicated that low expression of PARP1 and XRCC2 was associated with a better OS. Our preclinical experiments thus provide further evidence that a PARP-1 inhibitor (olaparib) may enhance the effect of RT on *XRCC2*-deficient CRCs.

Human tumor cell death following RT is caused mainly by the induction of DSBs, damage that can be repaired by HRR or NHEJ (27). We recently showed that XRCC2 deficiency sensitized CRCs to RT (5). However, not all XRCC2-deficient cancer cells were sensitive to IR *in vitro* (5, 27). IR induces complex DNA lesions that require repair *via* the HRR pathway (which depends on XRCC2), although the NHEJ pathway (which does not require XRCC2) can repair most of these lesions (27, 28). This might explain the differences in radiosensitivity in our HRR deficient model.

Radiosensitization by PARP-1 inhibitors such as olaparib is apparently mediated by inhibition of base excision repair, resulting in delayed repair of SSBs that, upon collision with progressing replication forks, are converted into 1-ended DNA DSBs. These DSBs can only be repaired by HRR (29). Supporting this model, PARP-1 inhibitors in combination with RT produced greater growth inhibition in BRCA2-deficient than in BRCA2-proficient breast cancers (30). Other studies reported that radiosensitization by PARP-1 inhibitors was enhanced in the presence of a variety of DNA DSB repair deficiencies, including those involving Ligase IV, and RAD51C (31, 32). Our results are consistent with these previous studies, in that olaparib treatment led to radiosensitization in CRC, particularly in tumors with XRCC2 deficiencies. Our *in vitro* studies of the effect of IR+olaparib indicated radiosensitization in XRCC2-deficient cell lines, manifested as decreased colony formation, increased γ-H2AX persistence, increased cellular senescence, and induction of cell cycle arrest. We also confirmed the effectiveness of this combination treatment *in vivo* using XRCC2-deficient tumor xenografts, which had delayed growth relative to xenografts with empty vectors.

We compared the extent of DNA breaks from IR alone *vs.* IR+olaparib by measuring the levels of γ-H2AX. As expected, this difference also correlated with residual levels of total DNA damage based on γ-H2AX

level. This result may be explained by the need to have repeated cycles of DNA synthesis, so that unrepaired single-strand DNA breaks (primarily caused by IR) are converted to DSBs which cannot be repaired because of XRCC2 deficiency. Cell cycle regulation is an important biological process also affected radiosensitivity, and cells are most sensitive to IR during the G2/M phase (33). There is evidence that PARP may promote G2/M arrest following genotoxic stress (34). Our data showed that IR+olaparib significantly increased the percentage of cells in G2/M phase compared IR alone and olaparib alone in CRC cell lines. Moreover, we observed a significant increase in XRCC2-deficient CRC cells after the combination treatment ($P < 0.01$; Figure 3A & B).

Promotion of cellular senescence can increase the effectiveness of RT (35). A previous study of the effect of a PARP-1 inhibitor combined with RT showed that radiosensitization manifested predominantly as prolonged growth arrest and senescence, with little or no contribution from apoptosis (36). Our results showed that IR+olaparib treatment led to significantly increased cellular senescence compared to either treatment alone, and the highest percentage of cellular senescence was in XRCC2-deficient cells. These results are in accordance with the study of Alotaibi et al., who demonstrated that PARP inhibitors did not increase radiation-induced apoptosis in DNA repair deficient tumor cells, but it did markedly enhance growth arrest and senescence (31). This lack of a role of apoptosis is not surprising, because RT is believed to mainly kill cells by induction of “mitotic catastrophe” (aberrant mitosis), in which there is a formation of large non-viable cells that have micronuclei or multiple nuclei (37, 38).

It is well known phospho-p53 activates a plethora of cellular responses, including the initiation of senescence and cell cycle arrest after IR (39, 40). Our results showed that olaparib+IR led to an increased level of phospho-p53 in XRCC2-deficient CRC cells. We also observed increased p21 levels in XRCC2-deficient CRC cells after IR; p21 is an inhibitor of cyclin-dependent-kinases and its induction by phospho-p53 leads to cell cycle arrest in G2/M. We showed that IR led to a massive arrest of the cell cycle in phase G2 that persisted 72 h after irradiation. In addition to its role in cell cycle arrest, p21 activation is also an initial step of accelerated senescence [41].

Conclusion

In summary, our preclinical study provides evidence that XRCC2 loss contributed to the therapeutic response of olaparib when combined with IR. These results demonstrated that olaparib may be a promising strategy for enhancing the radiosensitivity of advanced CRCs that have XRCC2 deficiencies.

Abbreviations

CRC: colorectal cancer; RT:radiotherapy; LARC:locally advanced rectal cancer ; neoCRT: neoadjuvant chemoradiotherapy; IR: ionizing radiation; NCCN: The National Comprehensive Cancer Network; OS: overall survival; XRCC2: Chinese hamster cells 2 gene; HRR: homologous recombination repair; DSBs: double-strand breaks; NHEJ: non-homologous end-joining; HRR: homologous recombination repair; β-gal:β-galactosidase.

Declarations

Acknowledgments

We thank the staff at the Department of Radiation Oncology in Huaihe Hospital of Henan University for their continuous help in carrying out radiation experiments.

Ethics approval and consent to participate

The animal studies and tissue blocks (No. HUSOM2016-26) were approved by the Institutional Ethics Review Board of the Huaihe Hospital of Henan University, China.

Consent for publication

All authors agree for publication.

Competing interests

The authors declare that they have no competing interests

Availability of data and materials

The data used and analyzed during this study are available from the corresponding author on request.

Author contributions

CJQ and XMS designed the experiments. ETZ and KWX provided advice on the experimental design and data presentation. CJQ, QYL and ZYJ performed the *in vivo* and *in vitro* experiments. HJ performed the immunostaining and analyses. CJQ and XMS analyzed the data and wrote the manuscript. All authors contributed to manuscript writing and editing.

Funding

This study was supported by grants from the National Natural Science Foundation of China (NSFC-U1504818), the Natural Science Foundation of Henan Province of China (182300410359), the Science and Technology Foundation of Henan Provincial (172102310152).

References

1. Siegel RL, Miller KD, Fedewa SA, Ahnen DJ, Meester RGS, Barzi A, et al. Colorectal cancer statistics, 2017. CA Cancer J Clin 2017;67(3):177-93.
2. van Gijn W, Marijnen CA, Nagtegaal ID, Kranenbarg EM, Putter H, Wiggers T, et al. Preoperative radiotherapy combined with total mesorectal excision for resectable rectal cancer: 12-year follow-up of the multicentre, randomised controlled TME trial. Lancet Oncol 2011;12(6):575-82.

3. Ma B, Gao P, Wang H, Xu Q, Song Y, Huang X, et al. What has preoperative radio(chemo)therapy brought to localized rectal cancer patients in terms of perioperative and long-term outcomes over the past decades? A systematic review and meta-analysis based on 41,121 patients. Int J Cancer 2017;141(5):1052-65.
4. Wang XC, Yue X, Zhang RX, Liu TY, Pan ZZ, Yang MJ, et al. Genome-wide RNAi Screening Identifies RFC4 as a Factor That Mediates Radioresistance in Colorectal Cancer by Facilitating Nonhomologous End Joining Repair. Clin Cancer Res 2019;25(14):4567-79.
5. Qin CJ, Song XM, Chen ZH, Ren XQ, Xu KW, Jing H, et al. XRCC2 as a predictive biomarker for radioresistance in locally advanced rectal cancer patients undergoing preoperative radiotherapy. Oncotarget 2015;6(31):32193-204.
6. Dedes KJ, Wilkerson PM, Wetterskog D, Weigelt B, Ashworth A, Reis-Filho JS. Synthetic lethality of PARP inhibition in cancers lacking BRCA1 and BRCA2 mutations. Cell Cycle 2011;10(8):1192-9.
7. Fong PC, Boss DS, Yap TA, Tutt A, Wu P, Mergui-Roelvink M, et al. Inhibition of poly(ADP-ribose) polymerase in tumors from BRCA mutation carriers. N Engl J Med 2009;361(2):123-34.
8. Pastwa E, Blasiak J. Non-homologous DNA end joining. Acta Biochim Pol 2003;50(4):891-908.
9. Helleday T, Lo J, van Gent DC, Engelward BP. DNA double-strand break repair: from mechanistic understanding to cancer treatment. DNA Repair (Amst) 2007;6(7):923-35.
10. Patel AG, Sarkaria JN, Kaufmann SH. Nonhomologous end joining drives poly(ADP-ribose) polymerase (PARP) inhibitor lethality in homologous recombination-deficient cells. Proc Natl Acad Sci U S A 2011;108(8):3406-11.
11. Loser DA, Shibata A, Shibata AK, Woodbine LJ, Jeggo PA, Chalmers AJ. Sensitization to radiation and alkylating agents by inhibitors of poly(ADP-ribose) polymerase is enhanced in cells deficient in DNA double-strand break repair. Mol Cancer Ther 2010;9(6):1775-87.
12. Verhagen CV, de Haan R, Hageman F, Oostendorp TP, Carli AL, O'Connor MJ, et al. Extent of radiosensitization by the PARP inhibitor olaparib depends on its dose, the radiation dose and the integrity of the homologous recombination pathway of tumor cells. Radiother Oncol 2015;116(3):358-65.
13. Bi Y, Verginadis, Il, Dey S, Lin L, Guo L, Zheng Y, et al. Radiosensitization by the PARP inhibitor olaparib in BRCA1-proficient and deficient high-grade serous ovarian carcinomas. Gynecol Oncol 2018;150(3):534-44.
14. Mukhopadhyay A, Elattar A, Cerbinskaite A, Wilkinson SJ, Drew Y, Kyle S, et al. Development of a functional assay for homologous recombination status in primary cultures of epithelial ovarian tumor and correlation with sensitivity to poly(ADP-ribose) polymerase inhibitors. Clin Cancer Res 2010;16(8):2344-51.
15. Tambini CE, Spink KG, Ross CJ, Hill MA, Thacker J. The importance of XRCC2 in RAD51-related DNA damage repair. DNA Repair (Amst) 2010;9(5):517-25.
16. Johnson RD, Liu N, Jasin M. Mammalian XRCC2 promotes the repair of DNA double-strand breaks by homologous recombination. Nature 1999;401(6751):397-9.

17. Zhang YZ, An JH, Liu YX, Wu XC, Han SS, Ren XQ, et al. XRCC2-Deficient Cells are Highly Sensitive to 5-Fluorouracil in Colorectal Cancer. Cell Physiol Biochem 2017;43(3):1207-19.
18. Azad A, Jackson S, Cullinane C, Natoli A, Neilsen PM, Callen DF, et al. Inhibition of DNA-dependent protein kinase induces accelerated senescence in irradiated human cancer cells. Mol Cancer Res 2011;9(12):1696-707.
19. Park Y, Chui MH, Suryo Rahmanto Y, Yu ZC, Shamanna RA, Bellani MA, et al. Loss of ARID1A in Tumor Cells Renders Selective Vulnerability to Combined Ionizing Radiation and PARP Inhibitor Therapy. Clin Cancer Res 2019;25(18):5584-94.
20. Xu K, Song X, Chen Z, Qin C, He Y. XRCC2 rs3218536 polymorphism decreases the sensitivity of colorectal cancer cells to poly(ADP-ribose) polymerase 1 inhibitor. Oncol Lett 2014;8(3):1222-8.
21. Redon CE, Nakamura AJ, Gouliaeva K, Rahman A, Blakely WF, Bonner WM. The use of gamma-H2AX as a biodosimeter for total-body radiation exposure in non-human primates. PLoS One 2010;5(11):e15544.
22. Redon CE, Nakamura AJ, Zhang YW, Ji JJ, Bonner WM, Kinders RJ, et al. Histone gammaH2AX and poly(ADP-ribose) as clinical pharmacodynamic biomarkers. Clin Cancer Res 2010;16(18):4532-42.
23. Krempler A, Deckbar D, Jeggo PA, Lobrich M. An imperfect G2M checkpoint contributes to chromosome instability following irradiation of S and G2 phase cells. Cell Cycle 2007;6(14):1682-6.
24. Zuckerman V, Wolyniec K, Sionov RV, Haupt S, Haupt Y. Tumour suppression by p53: the importance of apoptosis and cellular senescence. J Pathol 2009;219(1):3-15.
25. Lord CJ, Ashworth A. PARP inhibitors: synthetic lethality in the clinic. Science 2017; 355, 1152–1158.
26. Drucker L, Stackievitz R, Shpitz B, Yarkoni S.Incidence of BRCA1 and BRCA2 mutations in Ashkenazi colorectal cancer patients: preliminary study.Anticancer Res 2000;20(1B):559-61.
27. Zheng Z, Ng WL, Zhang X, Olson JJ, Hao C, Curran WJ, et al. RNAi-mediated targeting of noncoding and coding sequences in DNA repair gene messages efficiently radiosensitizes human tumor cells. Cancer Res 2012;72(5):1221-8.
28. Gerelchuluun A, Manabe E, Ishikawa T, Sun L, Itoh K, Sakae T, et al. The major DNA repair pathway after both proton and carbon-ion radiation is NHEJ, but the HR pathway is more relevant in carbon ions. Radiat Res 2015;183(3):345-56.
29. Karnak D, Engelke CG, Parsels LA, Kausar T, Wei D, Robertson JR, et al. Combined inhibition of Wee1 and PARP1/2 for radiosensitization in pancreatic cancer. Clin Cancer Res 2014;20(19):5085-96.
30. Evers B, Drost R, Schut E, de Bruin M, van der Burg E, Derksen PW, et al. Selective inhibition of BRCA2-deficient mammary tumor cell growth by AZD2281 and cisplatin. Clin Cancer Res 2008;14(12):3916-25.
31. Alotaibi M, Sharma K, Saleh T, Povirk LF, Hendrickson EA, Gewirtz DA. Radiosensitization by PARP Inhibition in DNA Repair Proficient and Deficient Tumor Cells: Proliferative Recovery in Senescent Cells. Radiat Res 2016;185(3):229-45.

32. Min A, Im SA, Yoon YK, Song SH, Nam HJ, Hur HS, et al. RAD51C-deficient cancer cells are highly sensitive to the PARP inhibitor olaparib. Mol Cancer Ther 2013;12(6):865-77.
33. Krempler A, Deckbar D, Jeggo PA, Lobrich M. An imperfect G2M checkpoint contributes to chromosome instability following irradiation of S and G2 phase cells. Cell Cycle 2007;6(14):1682-6.
34. 34.M Masutani , T Nozaki, K Wakabayashi, T Sugimura. Role of poly(ADP-ribose) polymerase in cell-cycle checkpoint mechanisms following gamma-irradiation.
Biochimie 1995;77(6):462-5.
35. Azad A, Bukczynska P, Jackson S, Haupt Y, Cullinane C, McArthur GA, et al. Co-targeting deoxyribonucleic acid-dependent protein kinase and poly(adenosine diphosphate-ribose) polymerase-1 promotes accelerated senescence of irradiated cancer cells. Int J Radiat Oncol Biol Phys 2014;88(2):385-94.
36. Gewirtz DA, Alotaibi M, Yakovlev VA, Povirk LF. Tumor Cell Recovery from Senescence Induced by Radiation with PARP Inhibition. Radiat Res 2016;186(4):327-32.
37. Roninson IB, Broude EV, Chang BD. If not apoptosis, then what? Treatment-induced senescence and mitotic catastrophe in tumor cells. Drug Resist Updat 2001;4(5):303-13.
38. Eriksson D, Stigbrand T. Radiation-induced cell death mechanisms. Tumour Biol 2010;31(4):363-72.
39. Fei P, El-Deiry WS. P53 and radiation responses. Oncogene 2003;22(37):5774-83.
40. 40.Bunz F, Dutriaux A, Lengauer C, Waldman T, Zhou S, Brown JP, et al. Requirement for p53 and p21 to sustain G2 arrest after DNA damage. Science 1998;282(5393):1497-501.
41. Ewald JA, Desotelle JA, Wilding G, Jarrard DF. Therapy-induced senescence in cancer. J Natl Cancer Inst 2010;102(20):1536-46.

Figures

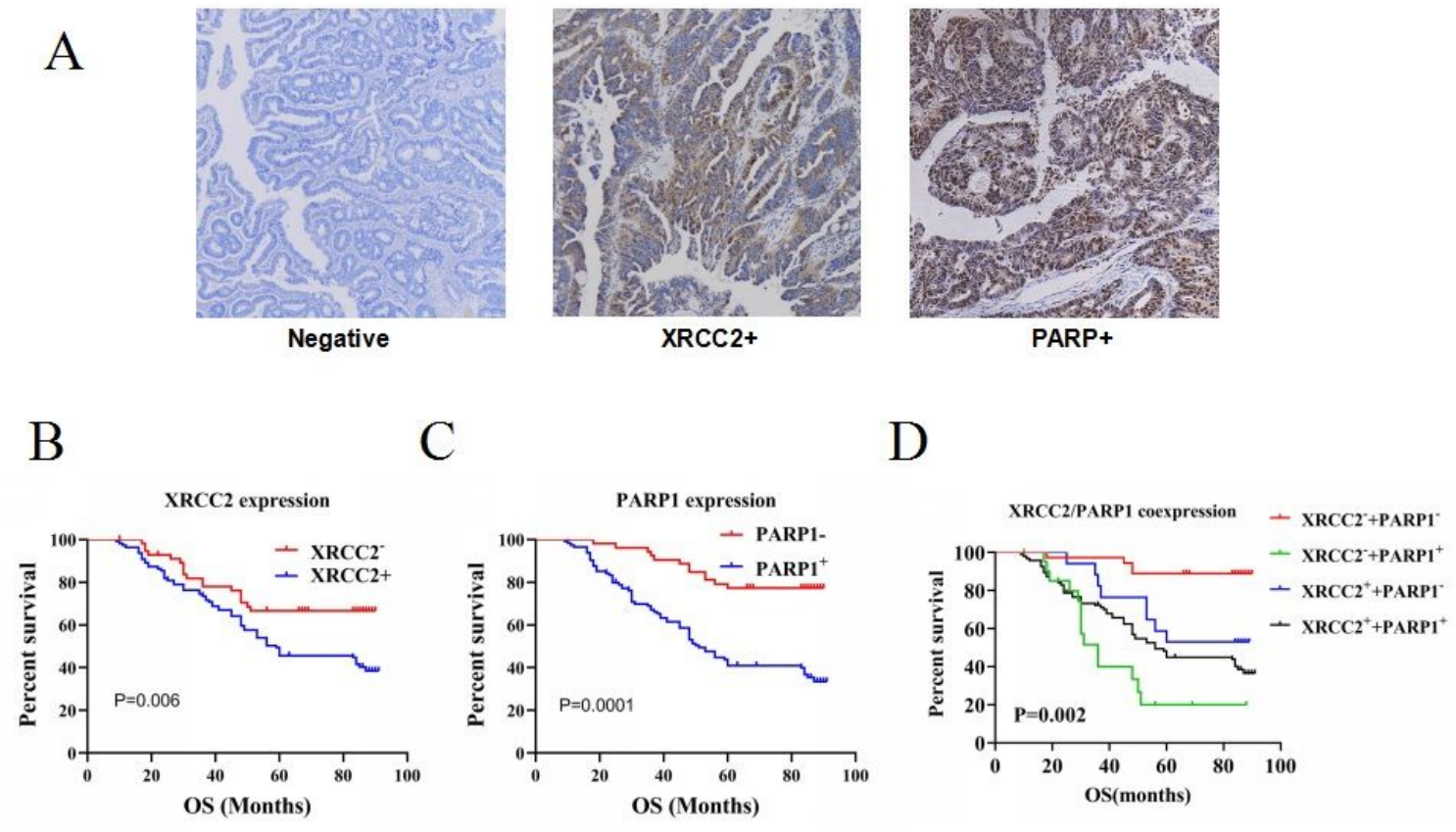

Figure 1

Prognostic significance of XRCC2 and PARP1 expression in LARC patients who received neoRT. (A) Representative immunohistochemical images showing the expression of XRCC2 and PARP1 in rectal tissues (×200). (B) Kaplan-Meier analysis of the effect of XRCC2 expression on OS. (C) Kaplan-Meier analysis of the effect of PARP1 expression on OS. (D) Kaplan-Meier analysis of the effect of XRCC2/PARP1 co-expression on OS.

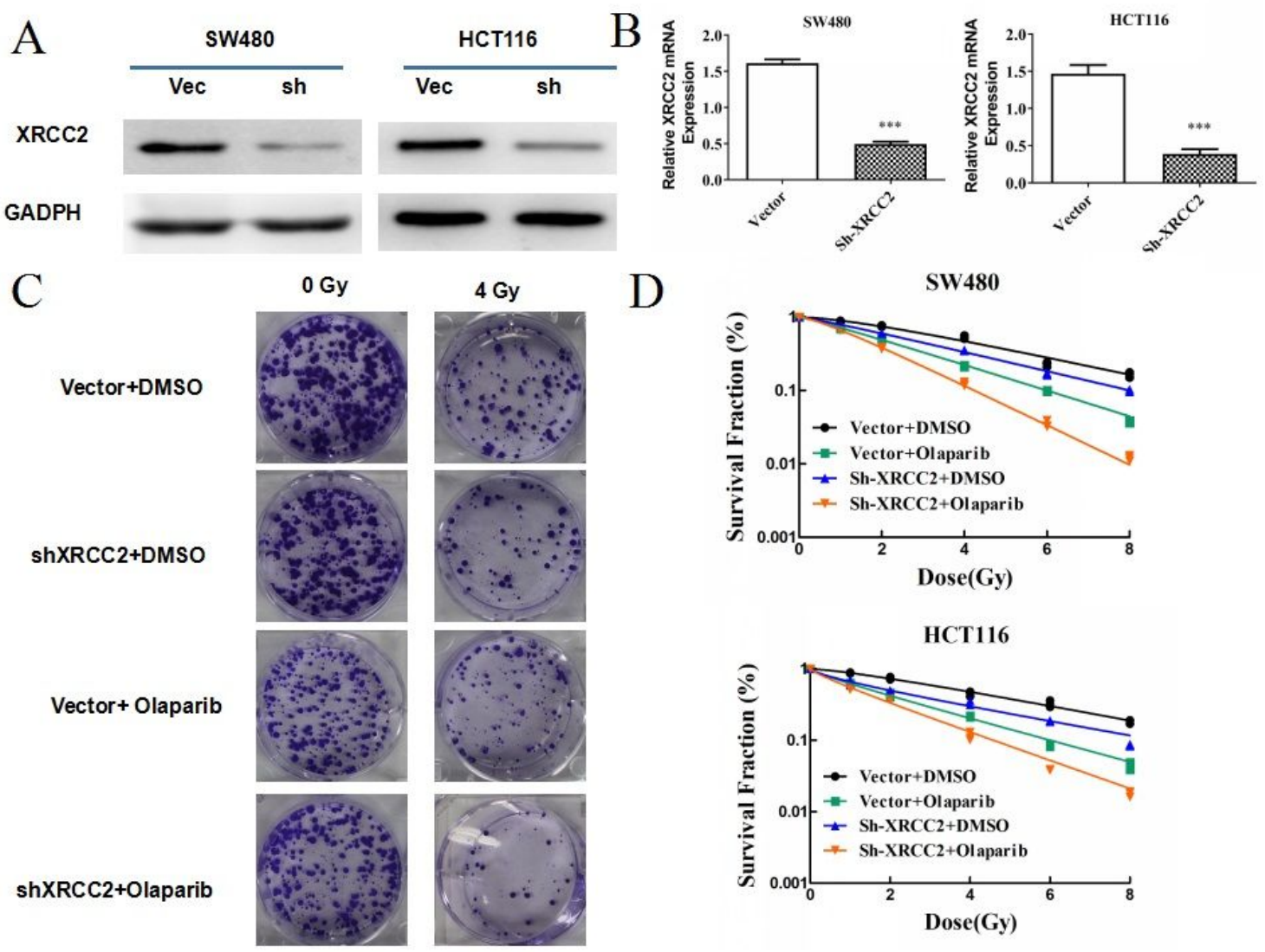

Figure 2

Effect of olaparib on the radiosensitivity of XRCC2-deficient rectal cancer cells. (A) Western blotting of XRCC2 in SW480 and HCT116 cells with (shXRCC2) and without (vector) XRCC2 knockdown. (B) qRT-PCR of XRCC2 in SW480 and HCT116 cells with (shXRCC2) and without (vector) XRCC2 knockdown. ***P < 0.001. (C) Representative images of the clonogenic cell survival assays in the different treatment groups. (D) Effect of IR dose on survival of cells in different groups. Lines are from statistical fits to the mean values from three independent experiments to a linear-quadratic (multi-target/single-hit) model.

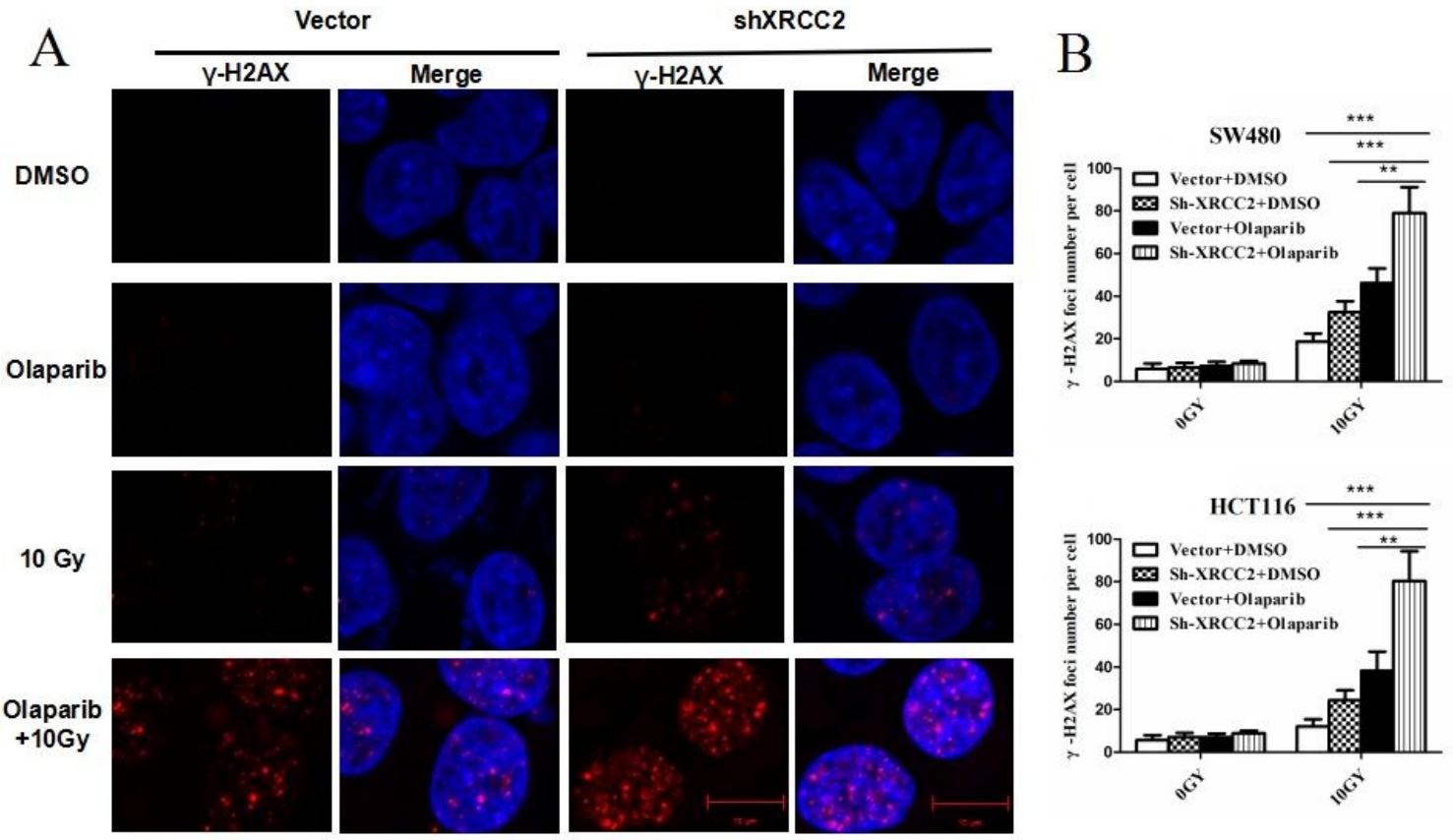

Figure 3

Effect of olaparib on the persistence of radiation-induced double-strand breaks in XRCC2-deficient rectal cancer cells. (A) Representative immunofluorescence images of γ-H2AX foci in SW480 cells at 48 h in the different treatment groups (×400). (B) Average number of γ-H2AX foci per nucleus in the different treatment groups. Results show the means and standard errors of the means (SEMs) from 3 independent experiments. **P < 0.01, ***P < 0.01).

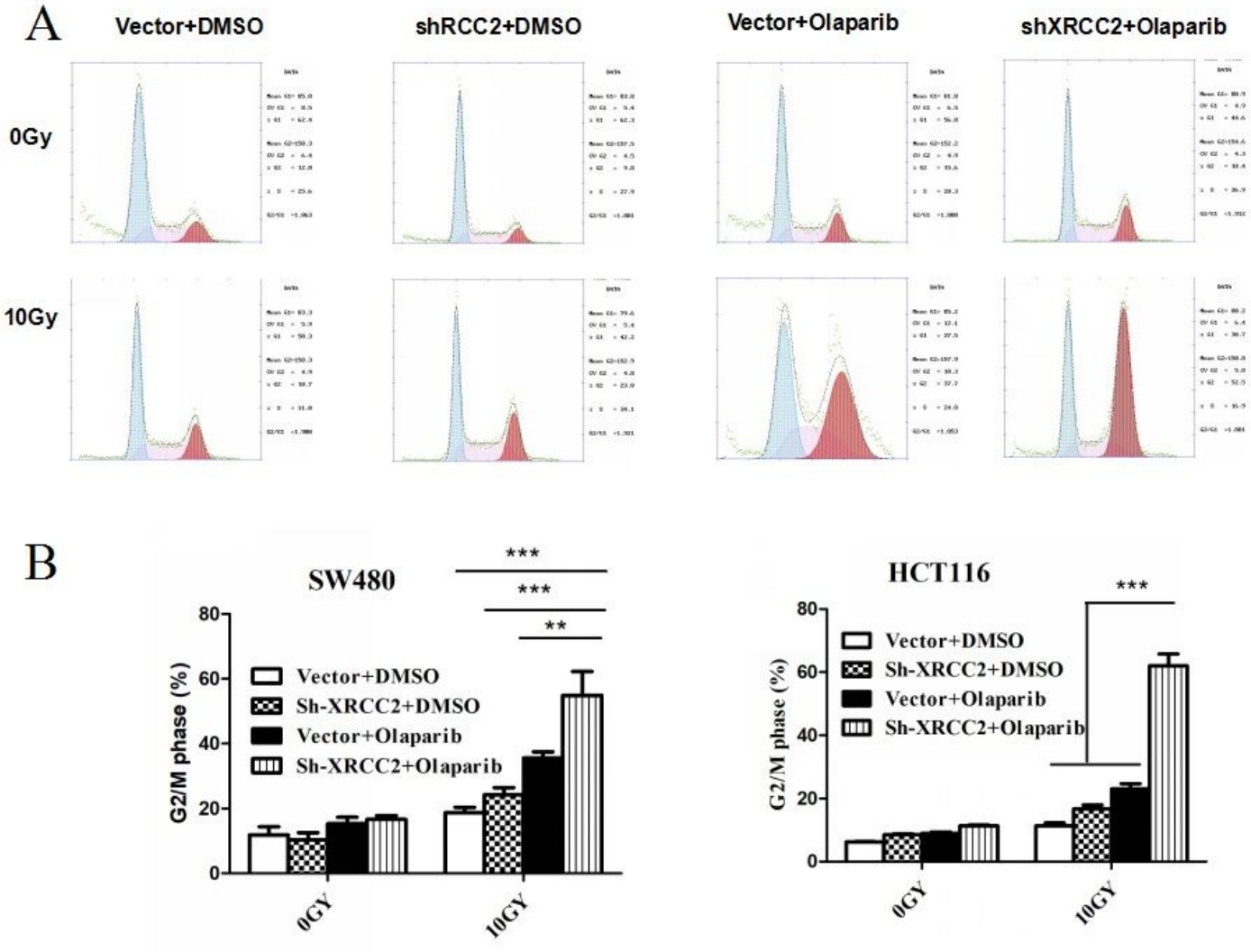

Figure 4

Effect of olaparib on sensitization of XRCC2-deficient cancer cells to IR-induced phase G2/M arrest. (A) Cell cycle profiles of cells with (sh-XRCC2) and without (vector) XCRCC2 knockdown at 48 h after the indicated treatment. (B) Quantification of flow cytometry results in the different treatment groups. Results show the means ± SDs from 3 independent experiments. **P < 0.01, ***P < 0.001.

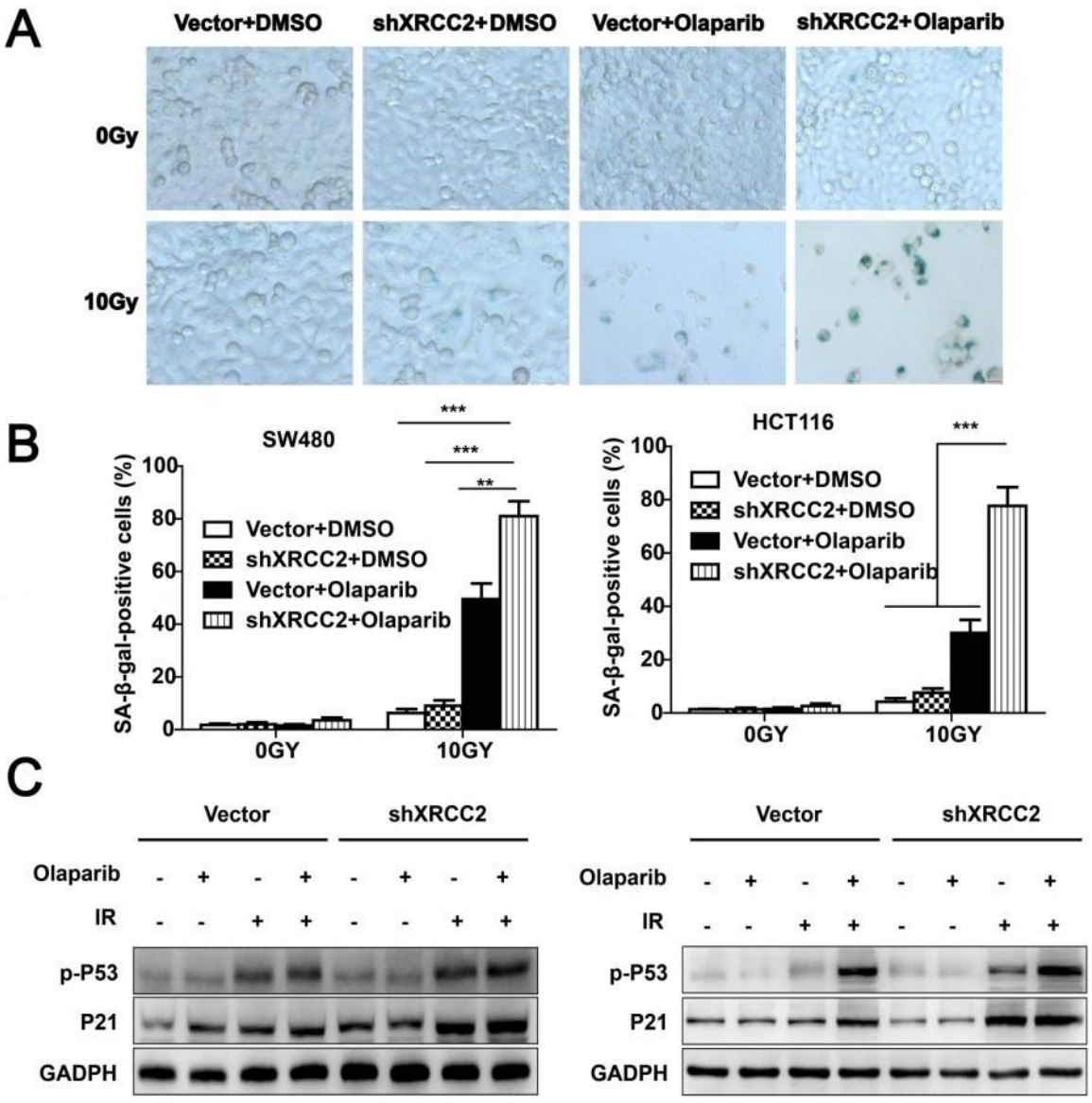

Figure 5

Effect of olaparib on senescence after in vitro IR treatment. (A) Representative images of senescence (β-gal activity) after 48 h in the different treatment groups (×40). (B) Quantification of microscopy results. Results show means ± SDs from 3 independent experiments. **P < 0.01, ***P < 0.001. (C) Representative western blotting of phospo-P53 and P21 in SW480 cells (left) and HCT116 cells (right) in the different treatment groups.

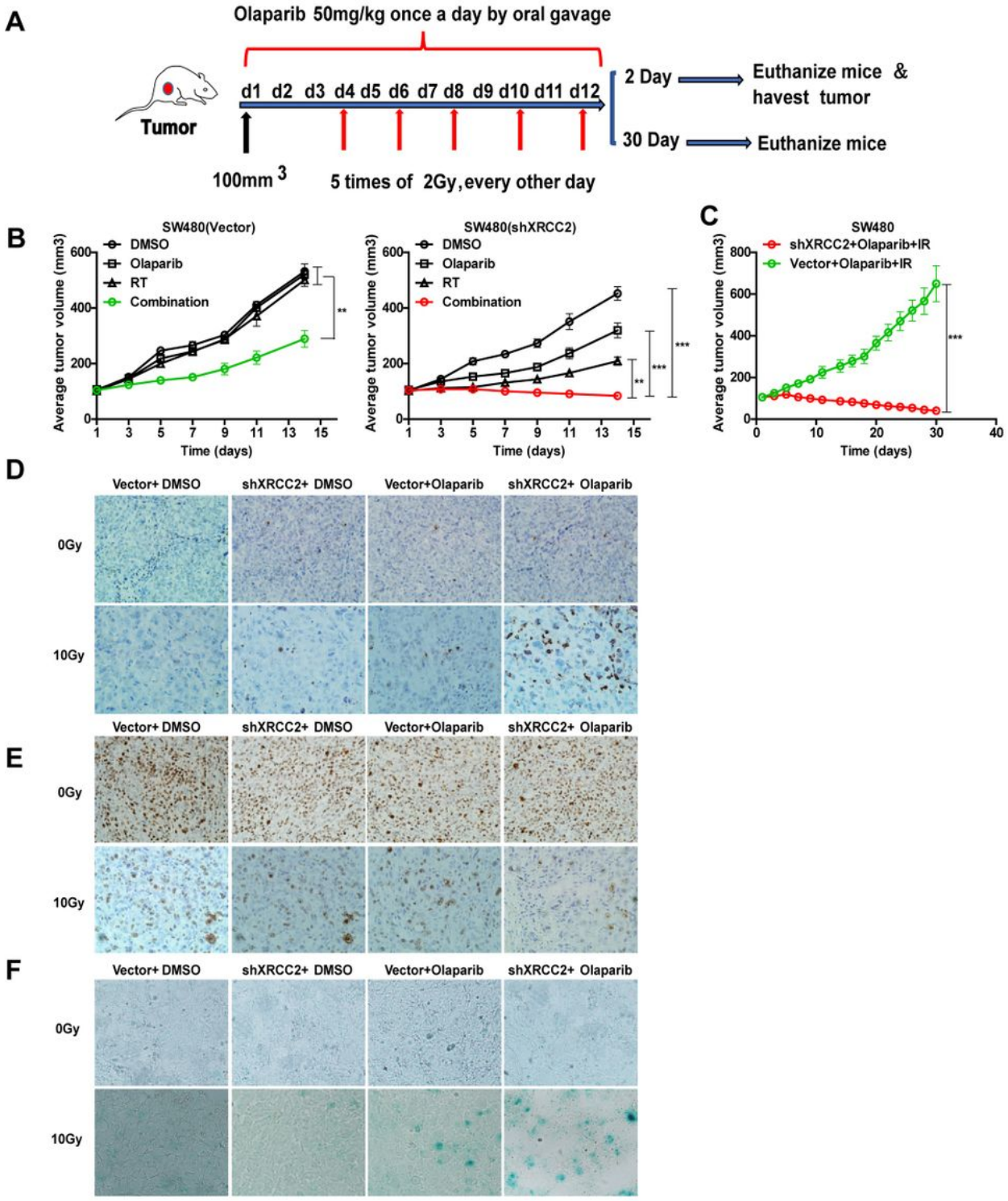

Figure 6

Effect of olaparib and IR on growth and senescence of XRCC2-deficient tumor xenografts in mice. (A) Experimental design. (B) Change of tumor volume over 2 weeks in the different groups that received SW480 cells with empty vectors (left) or shXRCC2 (right). Data are presented as means ± SEMs (n = 5); **P < 0.01, ***P < 0.001. (C) Change of tumor volume over 4 weeks in the two indicated groups. Data are presented as means ± SEMs (n = 5); ***P < 0.001. (D–F) Representative immunohistochemical staining

of γ-H2AX (top) and Ki67 (middle), and β-gal activity (bottom) in the different groups from tumors harvested 2 days after treatment with Olaparib with or without IR (×40).